

# On the applicability of the monodisperse medium model in numerical studies of flows in bubble columns

© A.S. Chernyshev, A.A. Schmidt

Ioffe Institute,  
194021 St. Petersburg, Russia  
e-mail: alexander.tchernyshev@mail.ioffe.ru

Received May 1, 2025

Revised August 12, 2025

Accepted August 17, 2025

A comparison of the results of a numerical study of flow in a bubble column using monodisperse and polydisperse approaches was conducted. It was found from the differences of the obtained solutions that, as bubble sizes increase to  $R_b > 1$  mm (corresponding to a Reynolds number for a bubble  $Re_b > 400$ ), both models are equivalent. It can be explained by a modification of the flow pattern associated with a change in the nature of the force interaction between the phases. Thus, efficient monodisperse medium models can be used to study flows with large bubbles.

**Keywords:** multiphase flows, polydispersity, numerical modeling.

DOI: 10.61011/TP.2025.12.62493.225-25

## Introduction

Multiphase flows and, in particular, bubble flows are an integral part of many natural and technological processes. Examples include gas bubbles rising from the seabed (as markers of deep deposits), satellite gas in the form of bubbles during oil production and transportation of an oil and gas mixture, chemical bubble reactors [1].

Polydispersity, as a rule, plays an important role in the formation of both the global structure of currents and the local properties of the flow [2]. Accounting for polydispersity in numerical modeling places higher demands on computing systems; however, it provides a detailed description of flows across a wide range of governing parameters.

Despite the fact that polydispersity is important for solving a wide range of problems about the flow of bubble media, the monodisperse approach is also actively used by researchers. For example, a calculation of a three-dimensional bubble column is presented in Ref. [3] within the framework of a monodisperse description, a comparison with experimental results demonstrated the applicability of the approach used.

The purpose of this study is to analyze the effect of polydispersity in the range of determining parameters of interest, the primary analysis of the causes of the decrease in the effect of polydispersity on the flow pattern, and the identification of a regime in which a monodisperse approach is possible.

## 1. Mathematical model

The model is based on the Eulerian-Eulerian approach to the description of multiphase flows (see, for example, [4]). Within the framework of this approach, the carrier (index  $l$ ) and dispersed (index  $b$ ) phases are considered as continuous

averages that fill the entire computational domain, at each point of which the volume content of the phase  $\alpha$  is set. In this case, the densities  $\rho$  of each of the phases are calculated as  $\alpha \cdot \rho_0$ , where  $\rho_0$  is the density of the substance of the corresponding phase.

Polydispersity is taken into account in the MULTiple SIZe Group (MUSIG) model. The model introduces a set of classes of monodisperse bubbles. A bubble size,  $R_{ib}$ , volume fraction  $\alpha_{ib}$  and velocity  $V_{ib}$  are determined for each class  $i$ , as well as an inherent system of momentum conservation equations and masses (the so-called heterogeneous MUSIG [5] model). The bubble size distribution is given by a piecewise constant function describing  $N$  classes (fractions) with constant bubble size [4].

The model is based on the equations of conservation of mass and momentum for the carrier and dispersed phases, taking into account the interphase force interaction, turbulence, and bubble dispersion [4]. The force interfacial interaction includes the buoyancy force  $F_{iB}$ , the Stokes force  $F_{iD}$ , the Saffman force  $F_{iL}$ , the force of attached masses  $F_{iVM}$  and the wall force  $F_{iWL}$ :

$$\begin{aligned} F_{iB} &= \alpha_{ib}(\rho_{ib} - \rho_l)g, \\ F_{iD} &= \frac{3\rho_l}{8R_{ib}} \alpha_{ib} C_{iD} V_{irel} |V_{irel}|, \quad V_{irel} = V_l - V_{ib}, \\ F_{iL} &= C_{iL} \alpha_{ib} \rho_l V_{irel} \times \text{rot} V_l, \\ F_{iVM} &= 0.5 \alpha_{ib} \rho_l \left( \frac{D_b V_{ib}}{Dt} - \frac{D_l V_l}{Dt} \right), \\ F_{iWL} &= -C_{iWL} \alpha_{ib} \rho_l |V_{irel} - (V_{irel} n_W) n_W|^2 n_W. \end{aligned}$$

Here  $g$  is the acceleration of gravity on the surface of the bearing medium,  $n_W$  is the normal to the nearest wall.

A correlation was proposed in Ref. [6] for the drag coefficient  $C_{iD}$  based on the Reynolds numbers  $Re_{ip}$  and Ertshem numbers  $Eo_i$ :

$$C_{iD} = \sqrt{C_D(Re_{ip})^2 + C_D(Eo_i)^2},$$

$$\begin{aligned} \text{Re}_{ip} &= \rho_l R_{ib} V_{ib} / \mu_l, \quad Eo_i = 4g(\rho_l - \rho_{ib})R_{ib}^2 / \sigma, \\ C_D(\text{Re}_{ip}) &= \frac{16}{\text{Re}_{ip}} \left( 1 + 2/(1 + 16/\text{Re}_{ip} + 3.315/\sqrt{\text{Re}_{ip}}) \right), \\ C_D(Eo_i) &= 4Eo_i / (Eo_i + 9.5), \quad Eo_i < 5. \end{aligned}$$

Here  $\mu_l$  is the dynamic viscosity of the bearing medium,  $\sigma$  is the surface tension coefficient.

The following expression is used for the coefficient  $C_{iL}$  [7]:

$$\begin{aligned} C_{iL} &= \min [0.288 \tanh(0.121 \text{Re}_{ip}), f(Eo_i)], \quad Eo_i < 4, \\ f(Eo_i) &= 0.00105Eo_i^3 - 0.0159Eo_i^2 - 0.0204Eo_i + 0.474. \end{aligned}$$

The coefficient  $C_{iWL}$  is calculated using the following formula [4]:

$$C_{iWL} = 0.47 \max \left\{ 0, \frac{1}{6.3} \cdot \frac{[1 - y_w/(20R_{ib})]}{y_w[y_w/(20R_{ib})]^{0.7}} \right\},$$

where  $y_w$  is the distance to the nearest wall.

The study uses the  $k-\omega$  SST model of turbulence [8] with additional source terms describing the generation and dissipation of turbulence due to the movement of bubbles relative to the carrier medium [4]. The effective viscosity of the carrier medium is calculated taking into account the Sato correction [9]. The dispersion of bubbles due to turbulent velocity pulsations in the carrier medium is taken into account using an additional diffusion term in the equations of conservation of the volume fraction of bubbles and their numerical density [4].

## 2. Numerical method

The proposed mathematical model was implemented as a program code using finite-volume approximation of equations on unstructured hexagonal grids. The second order of spatial accuracy was used to obtain a detailed picture of the flow and minimize the sampling error. To calculate the pressure fields and phase velocities, the SIMPLE algorithm was applied, adjusted for multiphase. The iterative process was organized using the pseudo-time method with the first order of accuracy. The model and numerical method were tested in detail, and a good agreement with the experiment was obtained (see [4]).

## 3. Setting the task

A series of calculations with a constant flow of bubbles is performed in this paper. The number of classes  $N = 1$  for the case of monodisperse bubbles. Based on the analysis conducted in Ref. [4], for the polydisperse case  $N = 10$ . The flow occurs in an axisymmetric bubble column with a diameter of  $D = 0.07$  m and a height of  $H = 0.65$  m due to the Archimedes force, bubbles enter from the bottom of the column and leave it from above through a free surface. The column is initially filled with water. The

gas in the form of bubbles enters the column through a coaxial axisymmetric aerator mounted in the bottom with a diameter of  $d = 0.05$  m. The gas parameters correspond to air under normal conditions. The ambient pressure corresponding to the pressure on the free surface is considered to be atmospheric, ambient temperature  $T = 297$  K, surface tension coefficient  $\Sigma = 0.072$  N/m (water-air).

## 4. Results

The simulation results in polydisperse and monodisperse formulations for the characteristic bubble size  $R_b$  0.25 and 1 mm are shown in Fig. 1. The normalized standard deviation of the desired value, calculated over the entire flow area, was used as a criterion for evaluating the difference between solutions obtained within the framework of polydisperse and monodisperse approaches. It can be seen that for bubbles with a size of 0.25 mm, the effect of polydispersity is significant (the criterion value is 10% for velocity and more than 60% for volume fraction and interfacial surface), while for bubbles of 1 mm, the criterion value is less than 1%.

The calculation of the equilibrium relative velocity of the bubbles  $V_{rel}$  was also carried out using an analytical zero-dimensional model based on the equation of the balance of interphase force interaction and buoyancy force:

$$\alpha_{ib}(\rho_{ib} - \rho_l)g = \frac{3\rho_l}{8R_{ib}} \alpha_{ib} C_{iD} V_{irel} |V_{irel}|.$$

The closing relations are taken from the complete mathematical model. The calculations showed good agreement with numerical experiments (Fig. 2) and the applicability of the analytical expression for flow analysis.

The study of changes in the nature of force interaction was conducted using an analytical model, the results are shown in Fig. 3. It can be seen that as the size of the bubbles increases, the influence of the individual components of the interfacial friction force changes. With small bubble sizes, viscous friction dominates on the surface of the bubble; with increasing size, the shape of the bubble becomes different from spherical, and the main contribution to the friction force is made by the component responsible for the deformation of the bubble.

## Conclusion

The analysis of the force interaction showed that when the bubble size  $R_b$  is of the order of 1 mm, the flow is rearranged, in particular, the nature of the friction force (Stokes) changes. For small bubbles, the main contribution to the Stokes force is made by viscous friction at the interface, and for large bubbles, the Stokes force is determined by the deformation of the bubble. The numerical simulation results are in good agreement with the predictions of the proposed analytical model for determining the equilibrium velocity of bubbles based on the balance of

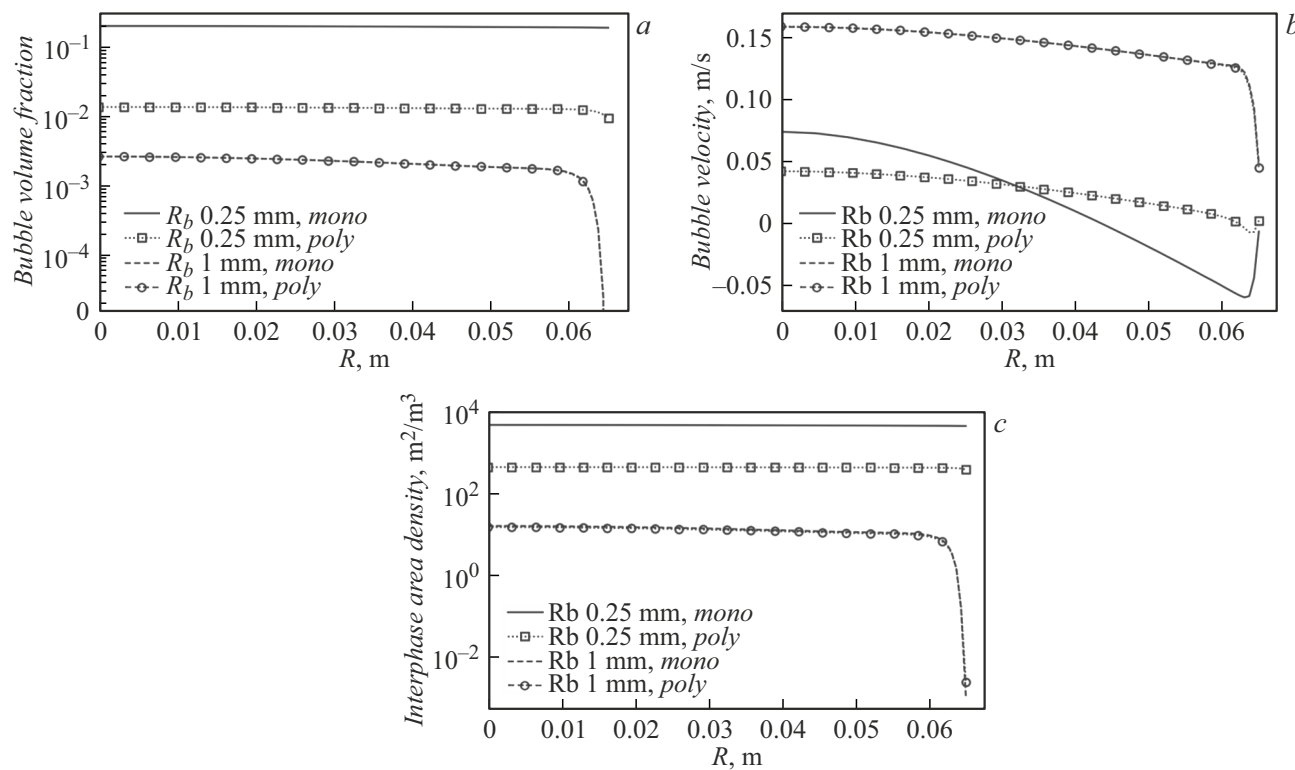


**Figure 1.** Distribution of the volume fraction of bubbles (a), bubble velocity (b) and the density of the interfacial surface area (c) in a cross-section 0.45 mm from the bottom m, using monodisperse and polydisperse approaches.

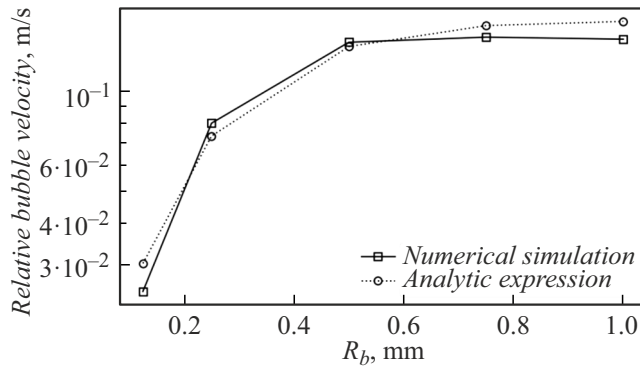


**Figure 2.** Comparison of the results of calculating the relative velocity of bubbles using numerical modeling and using an analytical expression.

interphase force interaction. A change in the nature of the force interaction of the phases with an increase in the bubble size leads to a decrease in the effect of the polydispersity of the bubble phase on the flow structure in column-type bubble reactors, which makes it possible to use economical models of a monodisperse medium.

## Acknowledgments

The article was completed as part of a Government assignment, subject number FFUG-2024-0005.

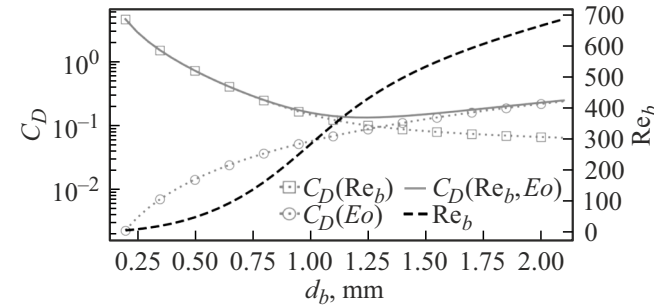


**Figure 3.** The change in the total Stokes force coefficient  $C_D(\text{Re}_b, \text{E}_o)$  depending on the bubble size  $d_b = 2R_b$ ; individual components describing the dependence on viscous friction  $C_D(\text{Re}_b)$  and on the shape of the bubble  $C_D(\text{E}_o)$  are given. The curve of the change in the Reynolds number of the bubble  $\text{Re}_b$  depending on the size of the bubble is shown.

## Conflict of interest

The authors declare that they have no conflict of interest.

## References

[1] F. Wang, N.D. Jin, D.Y. Wang, Y.F. Han, D.Y. Liu. Experimental Thermal and Fluid Science, **88**, 361 (2017). DOI: 10.1016/j.expthermflusci.2017.06.017

- [2] M.A. Pakhomov, V.I. Terekhov. *Tech. Phys.*, **60** (9), 1268 (2015). DOI: 10.1134/S1063784215090157
- [3] M. Raković, D. Radenković, A. Čočić, M. Lečić. *Advances in Mechanical Engineering*, **14** (4), 1 (2022). DOI: 10.1177/16878132221094909
- [4] A. Chernyshev, A. Schmidt, V. Chernysheva. *Water*, **15**, 778 (2023). DOI: 10.3390/w15040778
- [5] E. Krepper, D. Lucas, T. Frank, H.-M. Prasser, P.J. Zwart. *Nucl. Eng. Des.* **238**, 1690 (2008). DOI: 10.1016/j.nucengdes.2008.01.004
- [6] I. Roghair, Y.M. Lau, N.G. Deen, H.M. Slagter, M.W. Baltussen, M. Van Sint Annaland, J.A.M. Kuipers. *Chem. Eng. Sci.*, **66**, 3204 (2011). DOI: 10.1016/j.ces.2011.02.030
- [7] A. Tomiyama, H. Tamai, I. Zun, S. Hosokawa. *Chem. Eng. Sci.*, **57**, 1849 (2002). DOI: 10.1016/S0009-2509(02)00085-4
- [8] F.R. Menter, M. Kuntz, R. Langtry. *Heat Mass Transf.*, **4**, 625 (2003).
- [9] Y. Sato, K. Sekoguchi. *Int. J. Multiphase Flow*, **10**, 79 (1975). DOI: 10.1016/0301-9322(75)90030-0

*Translated by A.Akhtyamov*